Defence Science Journal, Vol. 66, No. 4, July 2016, pp. 381-390, DOI : 10.14429/dsj.66.10213

RESEARCH PAPER

Structure-property Characterisation at Nanoscale using *In-situ* TEM and SEM

Rajdeep Sarkar*, Chandan Mondal, Deepak Kumar, Sabyasachi Saha, Atul Kumar, and P. Ghosal

Defence Metallurgical Research Laboratory, Hyderabad - 500 058, India
**E-mail: rajdeep.sarkar@gmail.com*

ABSTRACT

In-situ electron microscopy is an emerging technique for real time visualisation of micro-structural changes of a specimen under some applied constraints inside microscope. In this study, *in-situ* nanoindentation experimentation on a carbon nanocoil inside transmission electron microscope has been reported. The elastic modulus of the carbon nanocoil is found to be 177 GPa. Similar experiments are also carried out on carbon nanotubes, but force response of carbon nanotubes is beyond the limit of sensors presently available. The *in-situ* dissolution behaviour of the secondary phases of a 7xxx series aluminum alloy under high vacuum condition in scanning electron microscope (SEM) in the temperature range of 350 °C to 400 °C has been reported. We report for the first time using *in-situ* SEM technique that dissolution of the $MgZn_2$-base phase present as eutectic and divorced eutectic forms could start at a temperature as low as 300 °C, although the usual homogenisation temperature of such alloys is always > 450 °C. Furthermore, the kinetics of dissolution of such phases, particularly when present in fine eutectic phase mixture, is significantly faster than what is observed under atmospheric pressure. It has been found that modification of surface composition under high vacuum condition plays a key role in the low temperature dissolution processes. It has further been found that the dissolution process does not start with the thinning of the inter-dendritic channels phase as proposed for Al-Zn-Mg-Cu alloys, rather it occurs by a combination of 'spheroidisation' and thinning process called 'the thinning, discontinuation, and full dissolution' mechanism. Results of the in-stu experiments under high vacuum are compared with the ex-situ dissolution experiments under normal atmospheric pressure.

Keywords: In-situ electron microscopy, scanning electron microscope, transmission electron microscope, Al-alloy, carbon nanocoil

1. INTRODUCTION

Correlation of microstructures with properties is very much important to understand the influence of structure on the properties of materials and their relationship to processing conditions. The understanding of these properties is important not only for the proper choice of material, but also for the design of new alloys with desirable properties for new technology. In recent years, several advanced materials and technologies have emerged where there is requirement for understanding of the mechanical behaviour in small volumes (sub-micron scale). But the characterisation of mechanical properties of materials in small volumes is a challenge to many existing testing and measuring techniques because of the difficulties associated with specimen fabrication and handling as well as extremely small loads and displacements involved in such cases. It should also be noted that mechanical behaviour of materials in small volumes cannot simply be deduced from the mechanical behaviour of bulk samples, because different physical/microstructural mechanisms dominate at different length scales. Therefore, it is important to measure the mechanical property of the materials at the length scale in which they are used in devices. Hence, suitable mechanical testing devices, which offer control at the appropriate micron to submicron scale, are necessary for testing on small volumes. Along with length scale of the material, time is an important parameter, which guides to study structural changes in small specimens or interplay between property/microstructure relationships in materials in real time. Recently, a few instruments or experimentation techniques, such as *in-situ* electron microscopy, have been developed with certain technologies to tackle above challenges. In this technique of *in-situ* electron microscopy, some form of active stimulus is applied to a sample inside electron microscopes (Transmission electron microscope or scanning electron microscope) during simultaneous imaging using a CCD able to operate at very fast rates (TV rate). This allows quantitative observations to be made of the micro-structural response (and in some cases material properties) to changing conditions. Common stimuli include thermal, mechanical, electrical, and magnetic, while less common (but demonstrated) stimuli include electrochemical, gaseous and liquid fluxes and optical irradiation[1].

Received : 08 May 2016, Revised : 26 May 2016
Accepted : 11 June 2016, Online published : 28 June 2016

1.1 *In-situ* Transmission Electron Microscopy

A powerful and unique approach has been developed by integrating the structural information of a material provided by TEM with the properties measured from the same material or with the conditions of structural changes by *in-situ* TEM[2-3]. This is also an ideal technique for understanding the property–structure relationship of individual nanostructures. Treacy[4],

et al. have measured Young's modulus of carbon nanotubes by *in-situ* TEM using quantitative analysis of the vibration amplitude from thermally induced vibration at the tips of the nanotubes. Wang[5-6], *et al.* have measured bending modulus of carbon nanotubes using electrically induced resonance of the tubes. For this study, they have used a dedicated specimen holder to apply a voltage across a nanotube and its counter electrode to induce electrostatic deflection or mechanical resonance. Bending modulus of carbon nanotubes was measured by applying an oscillating voltage and thereby inducing resonance to CNTs by tuning the frequency of applied voltage[5,7]. Mechanical properties of nanomaterials have also been measured using *in-situ* nano-indentation in TEM[8], which offers an easy real-time method to observe the response of the internal structure of a material during the indentation process. Dislocation nucleation, propagation, and interaction, as well as crack formation and phase transformations under applied load, are all easily observable. Wall and Dahmen[9] have developed an *in-situ* nanoindenter holder for studying deformation response of materials (silicon) in real time. Stach[10], *et al.* have improved the holder developed by Wall and Dahmen to enable accurate positioning control using the piezometric method with dedicated indentation capabilities to investigate the real time deformation behaviour of pure aluminum[10-11], titanium carbide[10] and silicon samples[10]. *In-situ* nano-indentation on an aluminum thin film has also been investigated by Jin[12], *et al*. to study grain boundary motion in response to the applied load. Jhonson[13] has used a commercially available nanoindenter holder, manufactured by Nanofactory Instruments AB, Sweden, for *in-situ* deformation study of chromium/scandium layers, sapphire and titanium-silicon-carbide. Besides *in-situ* mechanical property studies in TEM, several researchers have also studied micro-structural changes under external stimuli such as heating, chemical reaction[14], etc. While Ross[15] has reported crystal growth studies inside TEM, Saka[16] has studied solid-solid, solid-liquid, and solid-gas reactions in TEM. Zhou and Yang[17] have carried out oxidation studies using *in-situ* TEM.

1.2 *In-situ* Scanning Electron Microscopy

Like TEM, *in-situ* straining and heating experiments have also been carried out inside SEM chamber[18-19]. Motz[18] has reported several *in-situ* mechanical testing techniques for loading in tension, compression and bending modes in SEM. Testing under loading conditions of creep or cyclic fatigue with dwell times inside SEM chamber is also possible[18]. Besides, mechanical loading researchers have studied *in-situ* crystallisation, sintering, grain growth, corrosion, chemical reactivity etc. inside SEM chamber[19] in both hi-vacuum or in controlled atmosphere/environmental conditions. Most of these studies require *in-situ* heating experiments which involve heating of the samples with the help of a heating stage and continuous monitoring of the modifications of the specimens due to heating. In environmental scanning electron microscope (ESEM), along with the investigation of influence of temperature, heating rate and time on the sample, the effect of atmosphere compositions and variable pressure can also be studied. Researchers have also used electron back scattered diffraction (EBSD) in SEM along with *in-situ* loading and heating experimentation for identifying crystallographic orientation or any change in orientation of grains or phases under some external constraints. In case of both *in-situ* heating and loading experimentation, the specimen chambers of the SEMs should be large enough or be capable to accommodate the size and weight of the *in-situ* devices. Due to the presence of *in-situ* devices, it is not possible to work in smaller working distance which restricts the image resolution of the SEM. The image resolution of SEM further deteriorates while doing experimentation in high temperatures.

In this study, *in-situ* experimentation in both TEM and SEM has been reported. *In-situ* characterisation of the nanomaterials or bulk material through different techniques has been evolved due to certain needs. Nanotubes, nanofibres or nanocoils may be subjected to stresses and strains from the surrounding media during their service lifetime. Such stresses in the form of mechanical contact or thermal misfit may cause permanent deformation or even failure to the one-dimensional nanomaterials. Therefore, there is a need to characterize single nanomaterials. Mechanical properties of a nano-structured material have been estimated using *in-situ* transmission electron microscopy technique with the help of a TEM nanoindenter holder.

In-situ heating effect inside SEM has been studied on an Al alloy. In bulk alloys, such as Al alloy, homogenisation of the cast structure plays a critical role in hot working (rolling, forging, extrusion etc.) and subsequent precipitation heat treatments by removing the casting related compositional inhomogeneities and dissolving the coarse secondary alloy phases[20]. Although homogenisation of compositional inhomogeneties (usually called 'coring') involve bulk diffusion of the alloying elements, dissolution of secondary phases involves complex interaction between diffusion, surface energy, shape and distribution of secondary phases. Hence, understanding the dissolution mechanism poses more challenging task to the researcher[21-23]. Understanding the dissolution process of the low melting point secondary phases, such as eutectic and divorced eutectic $MgZn_2$-base phases situated mainly at the inter-dendritic channels (IDC) is, therefore, of considerable interest. Over the last several decades, significant progress has been made to the understanding of evolution mechanism and distribution control of strengthening precipitates. However, very little attention has been paid to some of the crucial industrial processes like homogenisation and its controlling mechanism. In this study, an attempt has been made to understand this phenomenon through *in-situ* techniques in SEM so that real time changes in the microstrcuture can be observed with heating and cooling of the sample. For this study, a 7xxx series aluminum alloy AA7055, having a nominal composition of Al-8Zn-2Mg-2.3Cu-0.15Zr, has been chosen, which is the highest strength Al alloy produced by ingot metallurgical route. The alloy finds widespread applications as aerospace structural material owing to its suitable combination of high specific strength, good fracture toughness and corrosion resistance[24-25]. Generally, alloys of the Al-Zn-Mg-Cu system are precipitation hardenable with G.P zones and precipitates being the effective hardening phases. At temperatures below the G.P. zone solvus, the precipitation sequence is widely accepted as:

Supersaturated solid solution G.P. zone (spherical) (platelets) h ($MgZn_2$) (plates /laths).

The as cast specimen of the AA7055 aluminum alloy shows a typical cored dendritic microstructure of primary α-Al solid solution surrounded by inter-dendritic secondary phases[26]. The predominant eutectic structure of the alloys is understood to be consisting of a 'quasi-binary reaction' products, evolving from parallel solidification of three quasi-binary eutectic reactions viz. α-Al / η[$MgZn_2$], α-Al / T[$Al_2Mg_3Zn_3$] and α-Al / S[Al_2CuMg][20]. Apart from being a part of eutectic structure, η-base phases are also present as 'divorced' phases. In order to understand the dissolution mechanism of eutectic and 'divorced'-eutectic phases at a chosen soaking temperature, the *in-situ* heating experiment is planned.

2. EXPERIMENTAL

2.1 *In-situ* Transmission Electron Microscopy

A SA2000 N TEM nano-indenter holder designed by the Nanofactory Instruments AB, Sweden was used for the *in-situ* nanoindentation inside TEM (FEI TECNAI 20T 200kV). Carbon nanotube (CNT), carbon nanocoil and a pure aluminum were chosen for *in-situ* nano-indentation experimentation in TEM.

Carbon nanocoil sample was prepared by focused ion beam (FIB) using a Quanta 200D (FEI) dual beam scanning electron microscope. Carbon nanocoils were first sonicated in methanol using ultrasonic vibrator. The nanocoils were subsequently dried and picked up by a copper wire of 0.25 mm diameter using conducting epoxy at the tip of the wire. Bundles of nanocoils attached to the Cu wire tip are shown in Fig. 1(a). After selecting a particular nanocoil, omniprobe™ was brought near to that coil (Fig. 1(b)) and was fixed with the coil using platinum deposition inside dual beam microscope as shown in Fig. 1(c). Once the coil was attached to the omniprobe, the other side of the coil was ion milled and the individual coil was fastened to the omniprobe (Fig. 1(d)). The omniprobe with the coil was then brought closer to the wire, which will be carrying the sample for loading in the nanoindenter holder. The nanocoil was welded to the wire using platinum deposit as shown by Figs. 1(e) - 1(f). Finally, the nanocoil sample from the omniprobe side was cut by milling to get a single nanocoil mounted on the wire and ready for the *in-situ* nanoindentation.

The wire containing the nano-coil was then screwed on a hat having legs (Fig. 2) to hold the wire and subsequently, the hat was placed on a ball in the TEM nano-indenter holder. Sample hat is connected to the piezo tube through the ball. This piezo tube guides the sample to move either left-right (X direction), up-down (Y direction), or forward-backward (Z direction), so that the sample can be brought near the indenter for loading. It must be stated here that unlike conventional nanoindentation or other indentation, the indenter is fixed in the TEM nanoindenter holder and sample moves towards the indenter. After loading the sample, Si based MEMS force sensor with mounted diamond tip indenter is placed in its position as marked in the holder. Once both the sample and sensor are loaded, proper alignment of the sample with respect to the indenter tip has to be done. Initial alignment is done in air i.e. outside the TEM, but under optical microscope. For sample alignment inside TEM, the indenter has to be brought within visible range by the movement of TEM stage. Then with piezo-controlled movement using the nano-indenter software, the sample of choice or particular position of the sample is brought close enough to the indenter i.e. within touching distance of the indenter, so that both the indenter and sample are visible at the same time. Before indentation, the sample and the indenter are aligned in such a way that both are at the eucentric height of the microscope. Though the *in-situ* experimentation part was similar for CNTs also, but CNT sample was prepared differently. CNTs were first dispersed by ultrasonication in methanol. Dispersed CNTs were then glued to the inner edge of a slotted grid using conduction epoxy as shown schematically in Fig. 3. Slotted grid with CNTs was bifurcated longitudinally in two halves and one of the halves was attached to the sample holder using conducting epoxy.

2.2 *In-situ* Scanning Electron Microscopy

A scanning electron microscope (EVO18, Zeiss, Germany) along with a heating stage (H1004 1250C heating module, Gatan, US) with intelligent temperature controller was used for *in-situ* scanning electron microscopy. Samples of 5 mm dia (or width) and of 7 mm height were polished using metallographic techniques before initiating the *in-situ* heating or cooling experiments. The polished sample was placed on the crucible of the heating stage inside SEM. The SEM imaging of the as-received sample was completed and particular locations were identified for carrying out the heating experiments. Subsequently, the heating module was switched on and the necessary temperature was set using the temperature controller. This temperature controller is used to accurately control and monitor the temperature. The temperature of the sample is monitored by thermocouple, which is mounted close to the sample, and the temperature is displayed on the temperature controller.

3. RESULTS AND DISCUSSION

3.1 *In-situ* Transmission Electron Microscopy

After aligning the carbon nanocoil and the Berkovich indenter perfectly inside TEM, the coil was brought to almost in contact with the indenter. Before initiating the indentation experiment or getting a force-displacement plot, detail of the spring constant of the indenter must be incorporated in the indentation software, as it is used for force calculation. During indentation, when load is applied to the diamond tip and sensor, the tip will move backwards, as the distance between the capacitor plates decreases and the force increases. Therefore the force obtained during force plot is related to the capacitance between two plates separated by a spring.

A depth or displacement controlled loading was used for the indentation of the nanocoil. Deflection of the coil due to indentation is shown in Fig. 4. Force-displacement, force-time, displacement-time plots for the same sample obtained during loading are shown in Figs. 5 (a) - 5(b). The force-displacement plot (Fig. 5(a)) shows that carbon nanocoil sample is elastically deformed, as the loading and unloading part of the curve follows the same path. Elastic modulus of the carbon nanocoil was estimated considering a cantilever type deflection at the

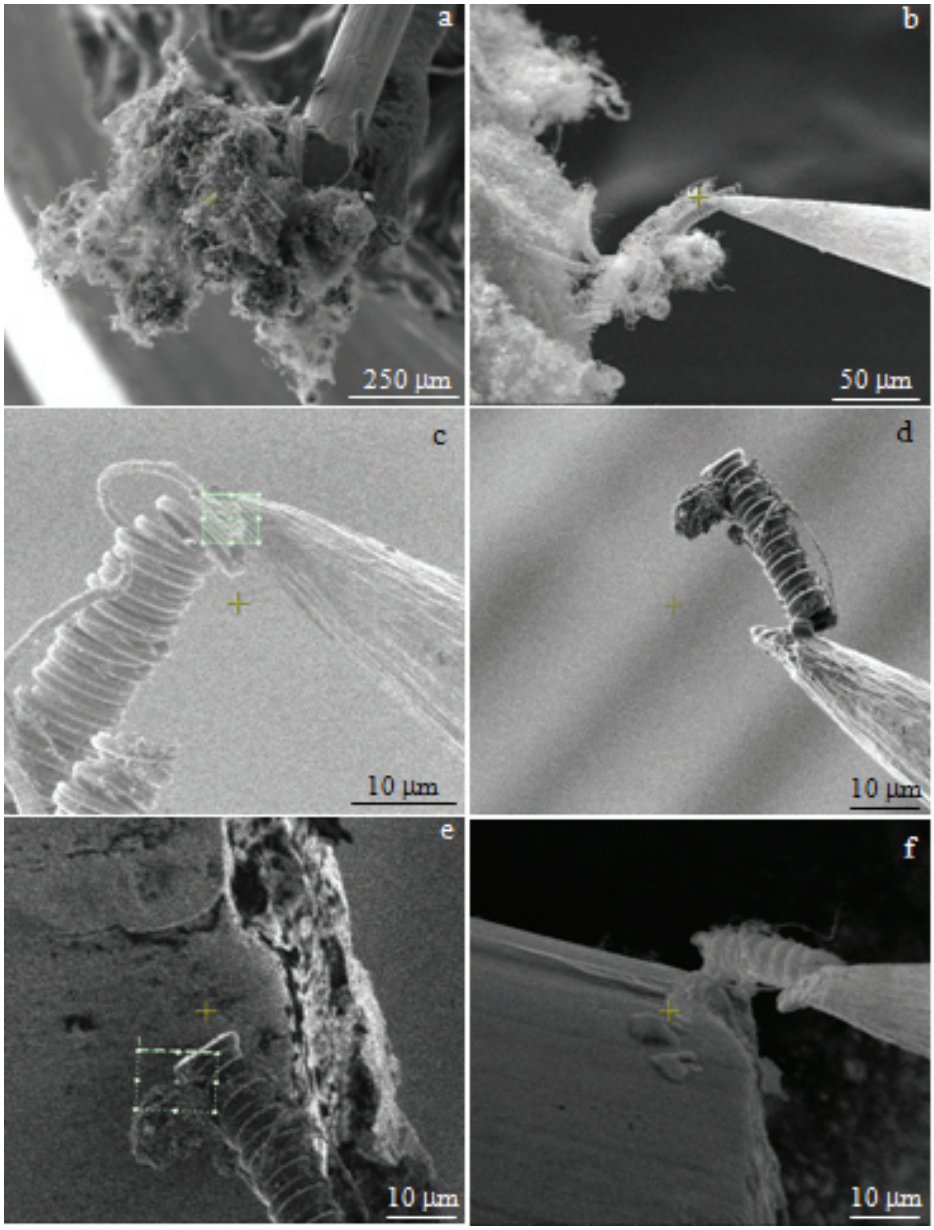

Figure 1. **SEM images of (a) bundles of nanocoils attached to a Cu wire tip, (b) omniprobe touching a coil, (c) welding of omniprobe with nanocoil using platinum deposition, (d) individual nanocoil hanging from omniprobe, (e)-(f) welding of the nanocoil with a wire which before loading in TEM nanoindenter holder.**

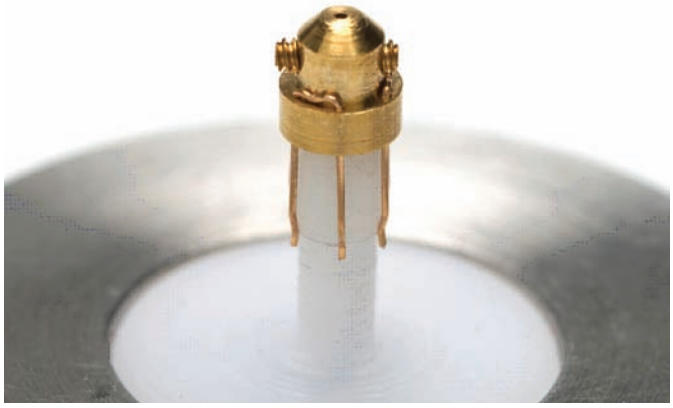

Figure 2. **Image of a typical hat stand for loading samples in TEM nanoindenter holder.**

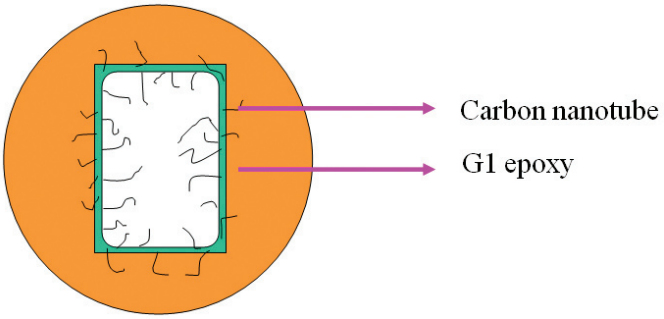

Figure 3. **Schematic view of CNT sample preparation for *in-situ* nanoindentation.**

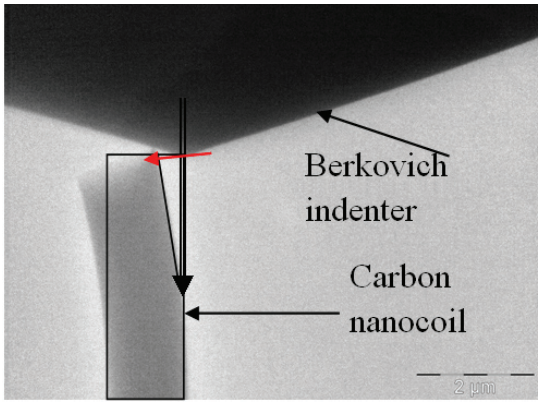

Figure 4. TEM image of a carbon nanocoil in contact with the Berkovich indenter during indentation; force resolved in a direction perpendicular to the coil axis for modulus determination.

displacement plot. Maximum values of force and displacement were considered and they were resolved in the perpendicular direction of the beam which was at 81º to the actual force direction. The resolved values of force and displacement were obtained as 0.378 µ*N* and 137 nm, respectively. Using all these data, the elastic modulus of the material was found as 177 GPa. The estimated elastic modulus value of the carbon nanocoil is found to be within the range of the modulus values reported in the literature for similar materials. Lawrence[27], *et al.* have carried out a 3-point bend test of a carbon nanofiber using AFM tip. While they have estimated the elastic modulus values of the carbon nanofibre within a range of 6 GPa - 207 GPa, Shaikjee and Coville[28] have reported the elastic modulus value of a carbon nanocoil as 100 GPa.

Similar to carbon nanocoil, multiwalled carbon nanotubes were also used for *in-situ* nanoindentation experiments. Though CNTs were dispersed before loading, it was observed in TEM

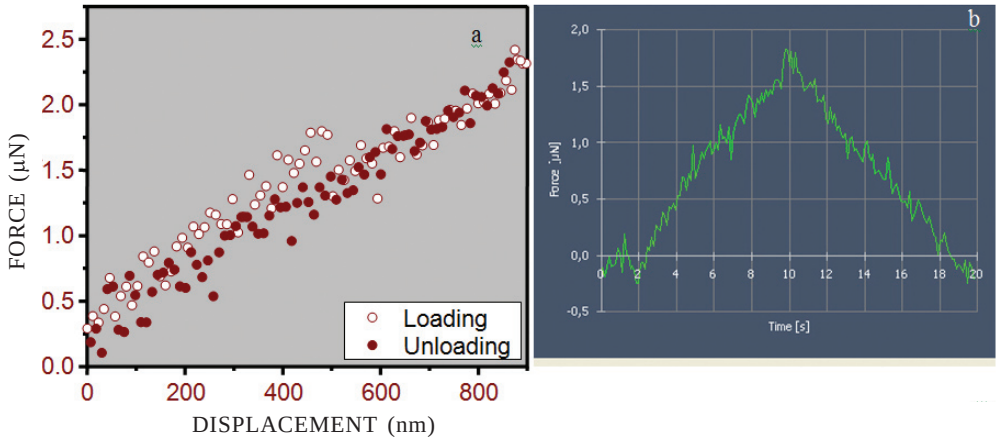

Figure 5. (a) Force-displacement and (b) force-time plots generated during *in-situ* nanoindentation of carbon nanocoil.

end of the beam in a direction perpendicular to the beam axis. It can be seen from Fig. 4 that force applied to the coil is not perpendicular to the end of the beam for determining modulus and the displacement obtained during nanoindentation test is also not in the direction perpendicular to the coil. Therefore the force and the displacement were resolved in the direction perpendicular to the coil as shown in Fig. 4 for necessary calculations. In the elastic regime, the Young's modulus of a cantilever type sample can be determined according to the following Eqn:

$$\delta = FL^3 / (3EI) \quad (1)$$

where δ is the deflection, F the applied load, L the length of the beam (coil here), E the Young's modulus and I the second moment of inertia. The second moment of inertia for a cylindrical beam of diameter d is:

$$I = \pi d^4 / 64 \quad (2)$$

therefore, using Eqns. (1) and (2), the Young's modulus E of a cylindrical cantilever is obtained as:

$$E = 64FL^3 / (3\pi\delta d^4) \quad (3)$$

The dimensions L and d were measured from the TEM images and were found as 30 µm and 1.3 µm, respectively. The force and displacement values were obtained from the force-

that they were in agglomerated form as it is very difficult to completely disperse CNTs. A single nanotube (Fig. 6) from the agglomeration was chosen for indentation. Berkovich indenter was used for indentation of CNTs. TEM images of the CNTs during indentation are as shown in Fig. 7 (a) - 7(d). Though bending of CNT due to loading was observed, but during the indentation no proper force plot was obtained. Indentation was

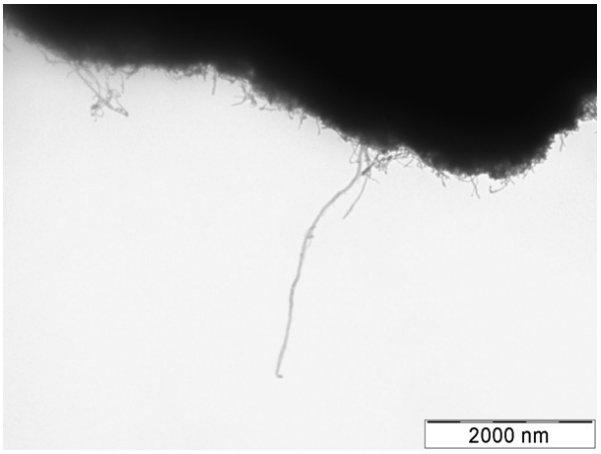

Figure 6. TEM image of individual CNT selected for *in-situ* nanoindentation.

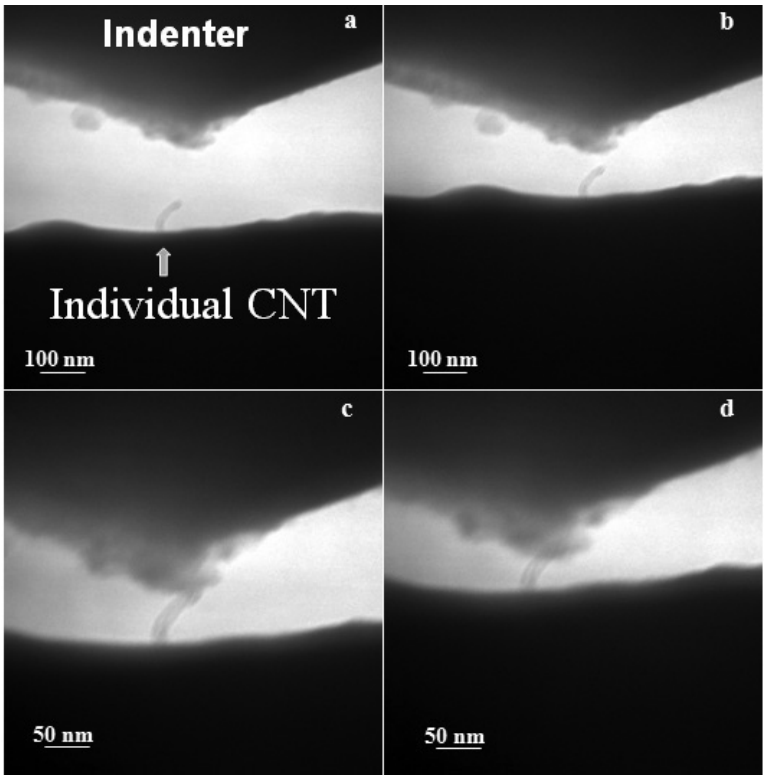

Figure 7. TEM images of CNTs during nanoindentation.

also tried on several nanotubes at the same time, but then also no increase in force was noticed. It might be due to the fact that the force responses of CNTs were in nano Newton range while the sensor capability is in micro Newton range. Therefore only scattered results were obtained during the experiment.

3.2 *In-situ* Scanning Electron Microscopy

In the in situ heating experiment of Al alloy, sequential evolution of phase morphologies have been observed at different time intervals during homogenisation at 350 °C - 400 °C. Although the actual homogenisation temperature of this alloy is 450 °C - 460 °C applied for 30 h - 35 h, we have attempted the experiments at a maximum temperature of 400 °C keeping in mind the capacity of the back scatter detector connected with the SEM. Figure 8 shows the in situ dissolution of eutectic-'divorced' eutectic combination at soaking temperature of 370 °C. The specimen has been heated in situ inside the SEM chamber at a slow rate of heating (~ 4.5 °C/min). Contrary to the findings of ex situ experiments by Eivani[22], *et al*., it could be seen that the dissolution process starts simultaneously with both the eutectic and divorced eutectic morphologies (Fig. 8 (c)-(d)).

However, morphological changes during dissolution of eutectic mixture and 'divorced'-eutectic phases appear to be different. The dissolution of lath-shaped divorced-eutectic phase, which is a Zn-rich $Mg(Zn,Cu,Al)_2$-based η phase[26], begins with perturbation-like discontinuous 'thinning' along the length of the phase (circle enclosed part of Fig. 8(d)). On the other hand, the dissolution of eutectic phase mixture (α-Al solid solution (dark) and $Mg(Zn,Cu,Al)_2$-based η phase (bright)) follows the classical 'spheroidisation' mechanism[29]. Recently, a specific dissolution mechanism called 'Thinning, discontinuation, and full dissolution (TDFD) has been forwarded by Eivani[22-23], *et al*. to account for the dissolution mechanism of grain boundary phases in Al-Zn-Mg alloy. The dissolution mechanism of the grain boundary phases with its intermediate stages is schematically illustrated in Fig. 9 as proposed by Eivani[22], *et al*. Through the proposed TDFD mechanism, Eivani[22], *et al*. have shown that the dissolution process starts with the thinning of the grain boundary phase without primary spheroidisation and the process continues until the phase becomes discontinuous. The present results suggest that the dissolution of divorced eutectic grossly follows the mechanism suggested by Eivani[22], *et al*., although at lower temperature of annealing (i.e., 370 °C) the discontinuation

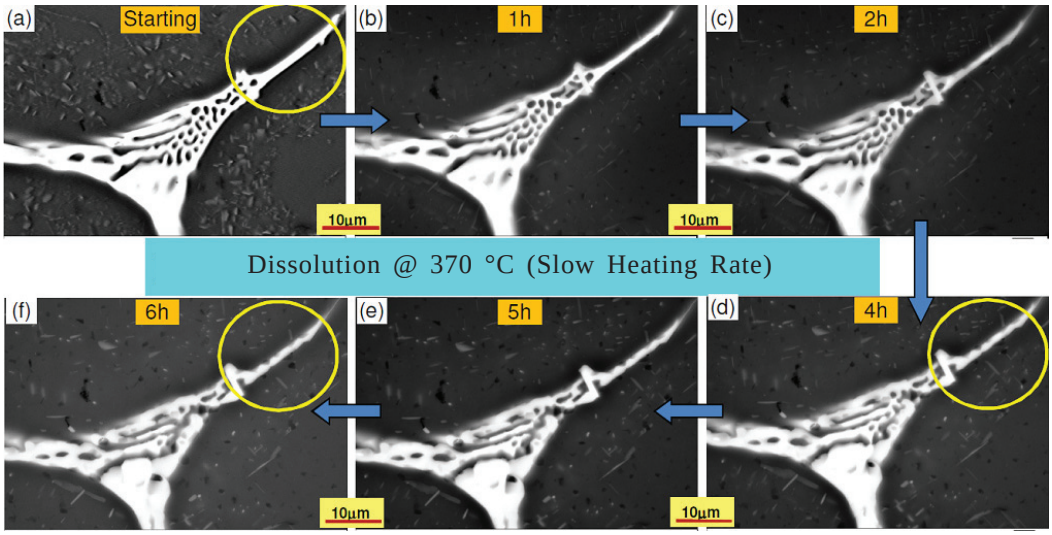

Figure 8. SEM images of microstructural development during *in-situ* heating at a soaking temperature of 370 °C. The specimen was heated up to the soaking temperature using a slow heating rate of 4.5 °C/min. Soaking time intervals are indicated in the each microstructure. Note the changes of the morphology of the divorced eutectic before dissolution.

could not be observed even after 24 h of soaking.

On the other hand, a distinct effect of heating rate could also be noticed in the present study. Figure 10 summarises the sequential morphological change of the as-cast structure when a higher (~ 15 °C/min) ramp rate has been used to reach the soaking temperature. It could be readily observed that the 'spheroidisation' of eutectic phase mixture starts even during the ramp heating when the specimen temperature reaches near 350 °C (Fig. 10(b). It could be further noticed that the dissolution of both eutectic phase mixture and 'divorced'-eutectic phase is complete during 3.5 h of soaking. However, the interesting observation is that the dissolution of divorced-eutectic in this case is dominated by 'thinning' as marginal/no surface perturbations could be noticed. The salient features of the phase dissolution by different heating rates are summarised as follows.

- Irrespective to the homogenisation temperature, fast heating leads to 'unusually' fast rate of secondary alloy phase dissolution of both 'eutectic' and 'divorced eutectic' morphologies,
- Effect of fast heating rate on dissolution kinetics is not widely known for high strength Al alloys, mechanism involved is also not well understood,
- Slow heating experiments reveal the morphological modifications of 'eutectic' and 'divorced eutectic' structures.

Further in situ experiments have been conducted at 400 °C.

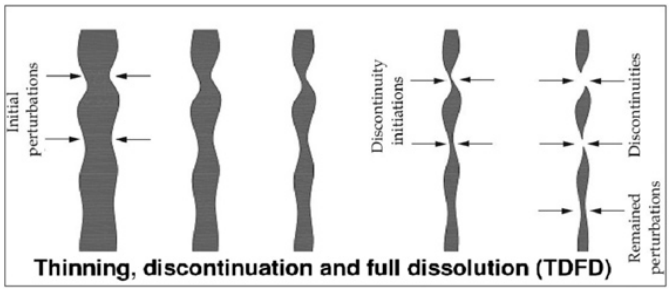

Figure 9. Schematic sequence of dissolution process as proposed by Eivani[20], *et al.*.

The results as displayed in Fig. 11 indicate a completely unexpected result. It is evident from the sequential micrographs that the dissolution is complete by ~ 25 min of soaking, compared to a commercial homogenisation schedule of 460 °C/30 h in air. To get insight into such extraordinary fast rate of dissolution kinetics, the in situ experiments are interrupted at different times and the chemical compositions of the phases are evaluated by energy dispersive spectroscopy (EDAX). It indicates that during soaking at 400 °C, the Zn content of the η-phase and the matrix vanishes rapidly such that the sample after complete dissolution of secondary phases shows negligible Zn content at the surface. This is consistent with the fact that the operating condition of the in situ experiment inside SEM chamber (~10^{-6} torr vacuum, 400 °C) coincides with the triple point of Zn. This further explains the relatively faster dissolution rate of the secondary phases at 370 °C with higher rate of heating. It is to be noted that during faster rate of heating, a temperature shoot up of 10 °C - 15 °C occurs at the beginning before the specimen temperature is brought to a stabilisation. Such a temperature shoot up enhances 'leaching' of Zn content from the system and it could possibly be responsible for dissolution of secondary alloy phases at a faster rate.

4. CONCLUSIONS

In-situ electron microscopy, which is an emerging technique for real time characterisation of a material, has been used in both TEM and SEM to experimentally evaluate two totally different objectives.

- *In-situ* nanoindentation which is a powerful technique for mechanical characterisation of individual nanostructures has been used for *in-situ* determination of modulus of a carbon nanocoil in TEM. The elastic modulus of carbon nanocoil has been determined experimentally and is found to be 177 GPa.
- Bending and elastic deformation of carbon nanotubes have been observed during loading and unloading of the CNTs using *in-situ* TEM nanoindenter holder. But, force response of carbon nanotubes (nano Newton) was found

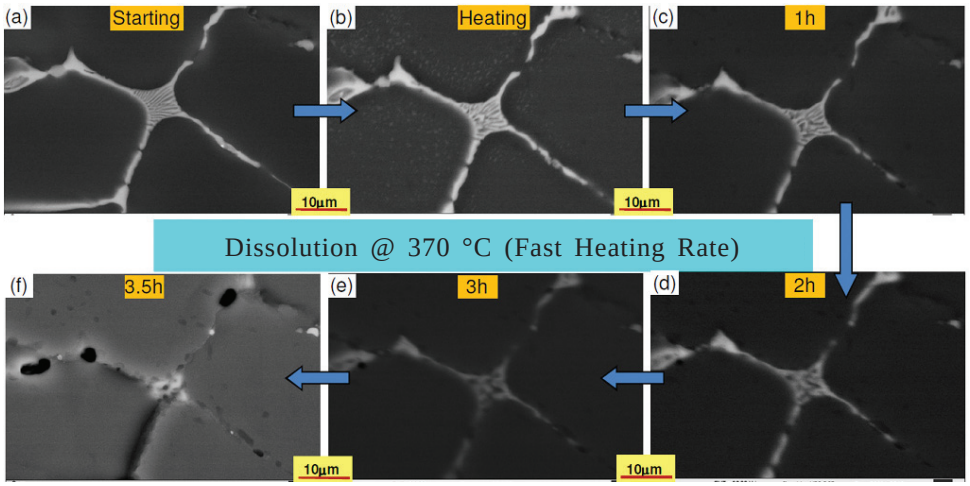

Figure 10. SEM images of microstructural development during in situ heating at a soaking temperature of 370 °C. The specimen was heated up to the soaking temperature using a faster heating rate of 15 °C/min. Soaking time intervals are indicated in the each microstructure.

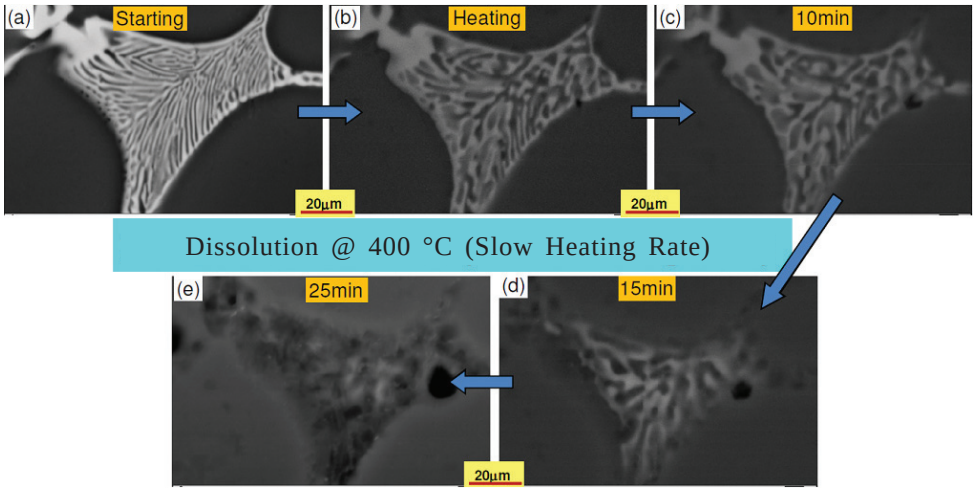

Figure 11. SEM images of microstructural development during in situ heating at a soaking temperature of 400 °C with a heating rate of 4.5 °C/min. Soaking time intervals are indicated in each microstructure.

to be below the limit of sensors (micro Newton).

- *In-situ* heating and homogenisation of as-cast AA7055 aluminum alloy specimen in SEM suggest that the dissolution behaviour of secondary alloy phases (eutectic and 'divorced-eutectic) grossly follows TDFD model at an intermediate temperature of soaking.
- Dissolution of 'divorced eutectic' is significantly sluggish compared to the eutectic phase mixture. Superfast dissolution of secondary phases near 400 °C under ultra high vacuum is associated with the 'loss' of Zn content of the phase.
- Slow heating experiments reveal the morphological modifications of 'eutectic' and 'divorced eutectic' structures.

REFERENCES

1. Stach, E. *In-situ* TEM – a tool for quantitative observations of deformation behavior in thin films and nano-structured materials. *In* Workshop on New Materials Science Enabled by *in-situ* Microscopies, DOE BES, September 13-15, 2001. http://escholarship.org/uc/item/8g6996zj
2. Wang, Z.L. *In-situ* mechanical properties of carbon nanotubes and nanowires. *In* Electron microscopy of nanotubes, edited by Z.L. Wang & C. Hui. Kluwer Academic Publishers, Netherland, 2003. pp. 165-189. doi: 10.1007/978-1-4615-0315-6_7
3. Wang, Z.L. Mechanical properties of nanowires and nanobelts. *In* Dekker Encyclopedia of Nanoscience and Nanotechnology, 2004, 1773-86.
4. Treacy, M.M.; Ebbesen, T.W. & Gibson, J.M. Exceptionally high Young's modulus observed for individual carbon nanotubes. *Nature*, 1996, **381**, 678-680. doi:10.1038/381678a0
5. Wang, Z.L.; Poncharal, P. & de Heer, W.A. Nano measurements of individual carbon nanotubes by *in situ* TEM. *Pure Appl. Chem.*, 2000, **72**(1–2), 209–19.
6. Wang, Z.L. New developments in transmission electron microscopy for nano technology. *Adv. Mater.*, 2003, **15**(18), 1497-1514. doi: 10.1002/adma.200300384
7. Tan, E.P.S. & Lim, C.T. Physical properties of a single polymeric nanofiber. *Appl. Phys. Lett.*, 2004, **84**(9), 1603–05. doi: 10.1063/1.1651643
8. Chen, X.; Zhang, S.; Dikin, D. A.; Ding, W.; Ruoff, R.S.; Pan, L & Nakayama, Y. Mechanics of a carbon nanocoil. *Nano Lett.*, 2003, **3**(9), 1299-1304. doi: 10.1021/nl034367o
9. Wall, M.A. & Dahmen, U. Development of an *in-situ* nanoindentation specimen holder for the high voltage electron microscope. *Microscopy Microanalysis*, 1997, **3**, 593-594.
10. Stach, E.A.; Freeman, T.; Minor, A.M.; Owen, D.K.; Cumings, J.; Wall, M.A.; Chraska, T.; Hull, R.; Morris, Jr. J.W.; Zett, A. & Dahmen, U. Development of a nanoindenter for *in-situ* transmission electron microscopy. *Microscopy Microanalysis*, 2001, **7,** 507–517.
11. Warren, O.L.; Shan, Z.; Asif, S.A.S.; Stach, E.A.; Morris, Jr., J.W. & Minor, A.M. *In-situ* nanoindentation in the TEM. *Mater. Today*, 2007, **10**(4), 59-60. doi: 10.1016/S1369-7021(07)70051-2
12. Jin, M.; Minor, A.M.; Stach, E.A. & Morris, J.W. Direct observation of deformation-induced grain growth during the nanoindentation of ultrafine-grained Al at room temperature. *Acta Mater.*, 2004, **52**, 5381–5387. doi:10.1016/j.actamat.2004.07.044
13. Johnson, L. Nanoindentation in situ a Transmission Electron Microscope. Department of Physics, Chemistry and Biology, IFM, Linköpings universitet, SE-581 83 Linköping, Sweden. Master's Thesis.
14. Sharma, R. Observing chemical reactions using transmission electron microscopy. *In In-situ* Electron Microscopy: Applications in Physics, Chemistry and Materials Science, edited by G. Dehm, J. M. Howe & J. Zweck, Wiley-VCH Verlag & Co. KGaA, Weinheim, Germany, 2012. pp. 145-169. doi: 10.1002/9783527652167.ch6
15. Ross, F. M. *In-situ* TEM studies of vapor- and liquid-

phase crystal growth. *In In-situ* Electron Microscopy: Applications in Physics, Chemistry and Materials Science, edited by G. Dehm, J. M. Howe & J. Zweck, Wiley-VCH Verlag & Co. KGaA, Weinheim, Germany, 2012. pp. 171-189.
doi: 10.1002/9783527652167

16. Saka, H. *In-situ* High-resolution observation of solid-solid, solid-liquid and solid-gas reactions. *In In-situ* Electron Microscopy at High Resolution, edited by F. Banhart, World Scientific Publishing Co. Pte. Ltd., Singapore, 2008.
17. Zhou, G. & Yang, J. C. *In-situ* TEM studies of oxidation. *in in-situ* electron microscopy: Applications in physics, chemistry and materials science, edited by G. Dehm, J. M. Howe & J. Zweck, Wiley-VCH Verlag & Co. KGaA, Weinheim, Germany, 2012. pp. 191-207.
doi: 10.1002/9783527652167.ch8
18. Motz, C. Mechanical testing with the scanning electron microscope. *In In-situ* Electron Microscopy: Applications in physics, chemistry and materials science, edited by G. Dehm, J. M. Howe & J. Zweck, Wiley-VCH Verlag & Co. KGaA, Weinheim, Germany, 2012. pp. 211-223.
doi: 10.1002/9783527652167.ch9
19. Podor, R.; Ravaux, J. & B. Henri-Pierre. *In-situ* experiments in the scanning electron microscope chamber. In Scanning Electron Microscopy, edited by Dr. Viacheslav Kazmiruk, InTech, 2012.
20. Sheppard, T. Extrusion of aluminium alloys. Kluwer Academic Publisher, London, 1999.
doi: 10.1007/978-1-4757-3001-2
21. Eivani, A. R.; Ahmed, H.; Zhou, J. & Duszczyk, J. Modelling dissolution of low melting point phases during the homogenisation of AA7020 aluminium alloy. *Mat. Sci. Technol.*, 2010, 26, 215.
doi:10.1179/174328409X399047
22. Eivani, A. R.; Ahmed, H.; Zhou, J. & Duszczyk, J. Evolution of grain boundary phases during the homogenization of AA7020 aluminum alloy. *Metall. Mater. Trans. A.*, 2009, **40**, 717.
doi: 10.1007/s11661-008-9741-9
23. Eivani, A. R.; Ahmed, H.; Zhou, J. & Duszczyk, J. Modeling the TDFD dissolution of Al–Fe–Mn–Si particles in an Al-4.5Zn-1Mg alloy. *Phil. Mag.*, 2010, **90**, 2865-2897.
doi:10.1080/14786431003662580
24. Lukasak, D.A. & Hart. R.M. Strong aluminum alloy shaves airframe weight. *Adv. Mater. Processes*. 1991, **140**(4), 46–49.
25. Cassada, W. Liu, J. & Staley, J. Aluminum alloys for aircraft structures. *Adv. Mater. Processes.*, 2002, **160**(12), 27-29.
26. Mondal, C. & Mukhopadhyay, A.K. On the nature of T($Al_2Mg_3Zn_3$) and S(Al_2CuMg) phases present in as-cast and annealed 7055 aluminum alloy. *Mat. Sci. Engg.*, 2005, A391, 367–376.
doi:10.1016/j.msea.2004.09.013
27. Lawrence, J.G.; Berhan, L.M. & Nadarajah, A. Elastic properties and morphology of individual carbon nanofibers. *ACS Nano*., 2008, **2**(6), 1230–1236.
doi: 10.1021/nn7004427
28. Shaikjee, A. & Coville, N. J. The synthesis, properties and uses of carbon materials with helical morphology. *J. Adv. Res.*, 2012, **3**, 195-223.
doi:10.1016/j.jare.2011.05.007
29. Ho, E. & Weatherly, G.C. Interface diffusion in the Al-$CuAl_2$ eutectic. *Acta Metall.*, 1975, **23**, 1451–1460.
doi:10.1016/0001-6160(75)90154-6

ACKNOWLEDGMENTS

The authors are thankful to SSPL, Delhi and DMSRDE, Kanpur for providing carbon nanotubes and carbon nanocoils, respectively for *in-situ* experimentation. The authors thank Director, DMRL, Hyderabad for his encouragement and permission to publish these results.

CONTRIBUTORS

Dr Rajdeep Sarkar has received his BE (Metallurgy) from REC (NIT), Durgapur, in 2003, MTech (Metallurgy) from Indian Institute of Technology, Kharagpur, in 2005, and PhD from Indian Institute of Technology, Kharagpur, in 2015. He is currently working as Scientist 'D' at at Defence Metallurgical Research Laboratory, Hyderabad. His fields of interests include: structure property correlation of Ti alloys, characterisation of super alloys, tungsten heavy alloys, nano-material etc.
In the current study, he has contributed in the experiments concerning in-situ indentation of carbon nanocoils in TEM and also drafted the manuscript.

Dr Chandan Mondal has received his BE (Metallurgy) from Jadavpur University, Kolkata, in 1998, ME (Metallurgy) from Indian Institute of Science, Bangalore, in 2000, and PhD from Indian Institute of Science, Bengaluru, in 2012. Currently working as Scientist 'E' at at Defence Metallurgical Research Laboratory, Hyderabad. His fields of interests includes: High strength aluminum alloys, crystallographic texture-processing-microstructure correlation, failure analysis of aero-engine components.
In the current study, he has contributed in the experiments concerning intermediate temperature homogenisation behaviour of high strength aluminum alloy through in situ annealing inside the SEM and also helped in drafting the manuscript.

Mr Deepak Kumar has received his BTech (Metallurgical Engineering) from Indian Institute of Metals, in 2014. He is currently working as a Technical Officer at Defence Metallurgical Research Laboratory, Hyderabad. His field of interest is characterisation of materials using different electron microscopy techniques.
In the current study, he has contributed by carrying out the sample preparation and subsequent *in-situ* heating experiments in SEM.

Mr Sabyasachi Saha has completed his BSc (Physics) from St. Stephens College, University of Delhi, in 2003. MSc (Physics) and M.Tech (Optoelectronics and Optical Communication) from Indian Institute of Technology, Delhi, in 2005 and 2007, respectively. Currently working as a Scientist in the Electron Microscopy Group at Defence Metallurgical Research Laboratory, Hyderabad. His research interests include, electron

microscopy and sample preparation using the dual beam SEM. He is currently also involved in characterisation of Gallium Nitride, wide band gap semiconductor material.
In the current study, he has contributed in sample preparation using FIB for *in-situ* nano-indentation experiments in TEM.

Dr Atul Kumar has received his MSc from Banaras Hindu University, in 1999, MTech from IIT, BHU, in 2002 and PhD in Materials Science and Engineering from Max Planck Institute for Metals Research, Stuttgart, Germany, in 2006. He is currently working as a Scientist in Mechanical Behaviour Group at Defence Metallurgical Research Laboratory, Hyderabad. His research interests include mechanical behaviour of materials at both bulk and at small length scale, shape memory alloys, residual stress and its gradient in MEMS and thermo-mechanical simulation using Gleeble.
In the current study, he has contributed in the in-situ indentation experimentation of carbon nanocoils in TEM and analyzed the results.

Dr Partha Ghosal has received his PhD from Indian Institute of Technology, Banaras Hindu University, in 1996. Currently, working as Head, Microscopy Group in the at Defence Metallurgical Research Laboratory, Hyderabad. He is working in the area of advanced characterisation techniques, along with SEM, EBSD, TEM and HRTEM. This includes *in-situ* mechanical testing and heating experiments of nano and advanced materials inside electron microscopes. Extensive electron microscopic works on Ti and W based alloys, nano-materials and nano composites is also carried out by him and in the scope of his interest.
In the current study, he has contributed in analysis of the results and given suggestions for carrying out different experiments.